[Supplementary Information]

Frontier performance of α-MnO_2 *in situ* dispersed over multi-walled carbon nanotubes covalently anchored to graphene oxide nanosheets framework as supercapacitor materials

Md. Mahinur Islam, M. Yousuf A. Mollah, Md. Abu Bin Hasan Susan and Md. Mominul Islam*

Department of Chemistry, University of Dhaka, Dhaka-1000, Bangladesh

*Corresponding author: mominul@du.ac.bd

1. Syntheses of composites

The methods followed for the functionalization of MWCNT and the synthesis of GMCNT ternary composites are described in main text of the article. The synthesis of GOM composite was carried out from graphite powder by following chemical method described elsewhere.[S1] Typically, 1.00 g of graphite and 0.50 g of $NaNO_3$ were first mixed together in a flask containing 50.0 mL H_2SO_4 (95%) kept in an ice bath. 2.67 g of solid $KMnO_4$ was then added to the suspension gradually. During addition, the mixture was stirred and the mixture was kept at room temperature with continuous stirring for about 2 h until the color of suspension turned to bright brown. Then 90 mL of distilled water was added. To achieve the desired composite, the temperature of the suspension was increased to about 100 °C and stirred for 12 h. The obtained mixture was allowed to settle down at room temperature and filtrated and finally washed with distilled water. After filtration and vacuum drying, the desired product was obtained in the form of black powder. Functionalization of MWCNT and the formation of composite involve following reactions: [34, 39, 44]

MWCNT (*s*) + conc. H_2SO_4 (*aq*) + conc. HNO_3 (*aq*)

$\rightarrow$ MWCNT–C(=O)–OH (*s*) + MWCNT–OH (*s*) + NO_2^+ (aq) + SO_4^{2-} (*aq*) (SI-1)

Graphite (*s*) + $NaNO_3$ (*aq*) + $KMnO_4$ (*aq*) + conc. H_2SO_4 (*aq*)

$\rightarrow$ GO(–OH) (*s*) + GO(O–O) (epoxy) (*s*) + MnO_2 (*s*) $\downarrow$ + NO_2^+ (*aq*) + HSO_4^- (*aq*) (SI-2a)

MWCNT-C=OOH (*s*) + GO(–OH) (*s*) + H^+ (*aq*)

$\rightarrow$ MWCNT–C(=O)–OGO (*s*) + H_2O (*l*) + H^+ (*aq*) (SI-2b)

2. Fabrication of composites-modified graphite electrodes and determination of C_{sp}

The prepared composites were deposited on clean, polished, smooth surface of a graphite disk electrode (diameter ca. 0.615 cm) that was tightly sealing a graphite rod with a shrinkable polymeric tube. Solid composite with weighted mass (0.05-0.07 mg) using a high precision 6-digit analytical balance (Model: GH-252, A&D, Japan) kept on an anti-vibration table in a silent place. 5% PVDF were taken in glass vial containing 1000 µL DMSO. This mixture was sonicated in an ultrasonic bath for 1 h and the dispersed solid mass was deposited on a flat electrode surface by solution casting method, where the suspension was added drop wise. After natural evaporation of DMSO, the prepared electrode was dried overnight at 100 °C in a vacuum oven. Similar method was followed for preparing MnO_2/GO binary composite modified graphite electrodes.

Using the discharging time of the GCD responses, the value of C_{sp} (in F/g) was determined by following the equations given below:

$$C_{sp} = \frac{i \times \Delta t}{\Delta V \times m} \quad \text{(SI-3)}$$

where, i is the current in ampere (A), Δt is the discharge time in second (s), ΔV is the potential difference in volt (V) and m is the mass of active material in gram (g). The corresponding energy density, E_{energy} (in W h kg^{-1}) and power density P (in W kg^{-1}) were determined by using the following relationships:

$$E_{energy} = \frac{C \times \Delta V^2}{2 \times 3600} \quad \text{(SI-4)}$$

$$P = \frac{E_{energy}}{t} \quad \text{(SI-5)}$$

where, t is the time of discharge stage in h and the other symbols have their meanings (*vide supra*).

3. Fourier-transform infrared (FTIR) spectroscopy

Vibrational spectra of the samples were recorded with Perkin Elmer (Model: HIMADZU, Japan) FTIR spectrophotometer in the range of 400–4000 cm^{-1}. FTIR measurement of the sample was carried out in a KBr pellet, the weight ratio of sample: KBr was around 200 : 1. About 200 mg KBr and 1-2 mg of synthesized/functionalized composite were mixed, grinded homogeneously and pressed to make a pellet. Background correction was done with a pure KBr pellet to avoid the contribution of infrared active atmospheric gases such as CO_2 and H_2O vapor in the spectra of samples. Fig. SI1 represents the FTIR spectra of GMCNT-5, GMCNT-10, GMCNT-30 and GMCNT-50. A broad band of 3300–3600 cm^{-1} corresponds to the stretching and bending vibration of -OH group of water molecule.

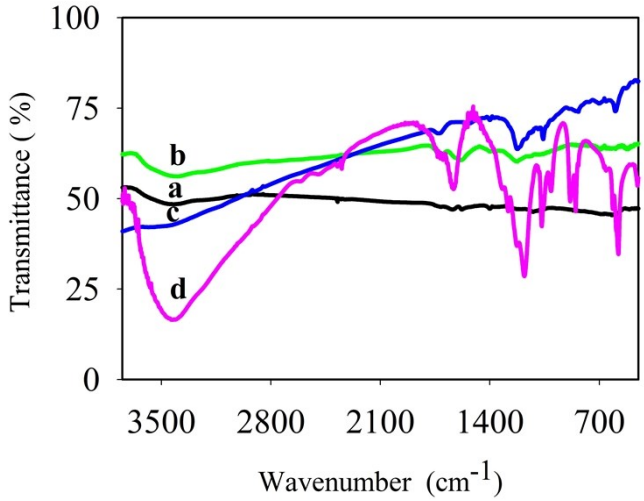

Fig. SI1: FTIR of **(a)** GMCNT-5, **(b)** GMCNT-10, **(c)** GMCNT-30 and **(d)** GMCNT-50.

The Mn-O stretching band is observed at 601 and 619 cm^{-1} for GMCNT-5 and GMCNT-10, respectively, but that was observed at 595 and 587 cm^{-1} for GMCNT-30 and GMCNT-50, respectively.[S2] This is the evidence of MnO_2 formation in these composites, which is also confirmed by the characteristic peaks in XRD and EDS responses. The presence of oxygen containing functional group in both composites were confirmed by the bands of $\upsilon_{C=O}$ at 1720 and 1740 cm^{-1}, $\upsilon_{O\text{-}H\ deform}$ at 1410 and 1405 cm^{-1}, $\upsilon_{C\text{-}O}$ at 1220 and 1235 cm^{-1} for GMCNT-5 and GMCNT-10 .[S3,S4] A reduction in the intensity for the oxygen containing groups could be seen for GMCNT-5 (Fig. SI1). The band at 1620 cm^{-1} observed for all the composites is attributed to C=C aromatic group [S4] and the relative intensity increases with increasing the percent of MWCNT. The interaction between GO and F-MWCNT occurs through the intermolecular hydrogen bond.[S5] The extent of such interaction depends on the

efficiency of insertion of F-MWCNT in between GO nanosheets achieved during the *in situ* exfoliation process; best achieved at 15 % of F-MWCNT insertion.

4. Field emission scanning electron microscopic (FESEM) analysis

The surface morphology and microstructure of the prepared composites were characterized by FESEM analysis and using an image processing program (ImageJ 1.51k, Java 1.6.0-24 (64-bit), USA). The number of definite size particles with surface area and perimeter were calculated from the experimental images. All of FESEM images representing the morphologies of synthesized composites (left column) and the corresponding mapped images (right column) are shown in Figs. SI2 to SI4. The mapping of particles presents was carried out in the scale of 1 to 100 nm. The red points in the mapped images represent size, shape and locations of the particles. The different parameters representing the morphologies of the synthesized composites determined using ImageJ are compared in Fig. SI4 (c).

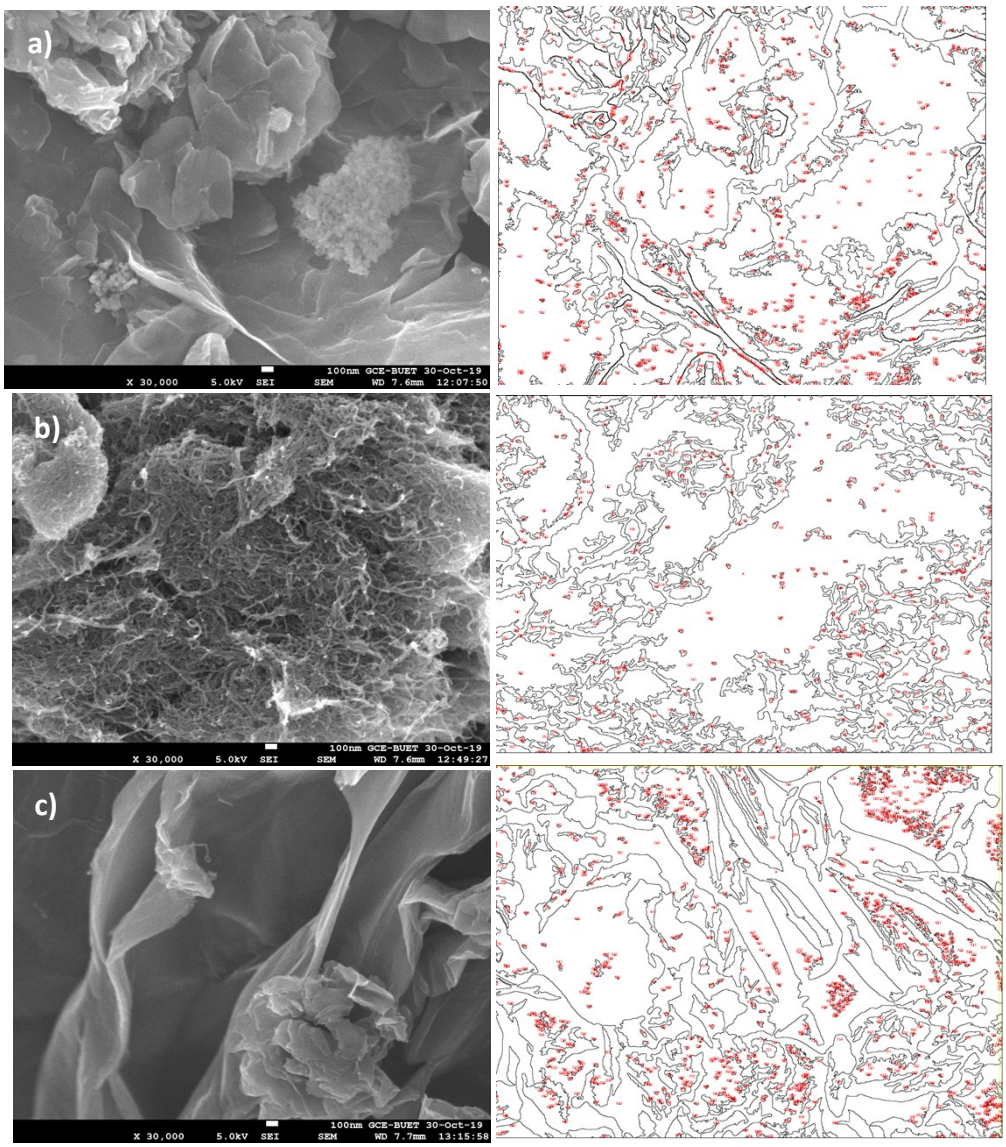

Fig. SI2: Experimental FESEM image of **(a)** GOM, **(b)** F-MWCNT and **(c)** GMCNT-5. Right side images are the corresponding mapped images.

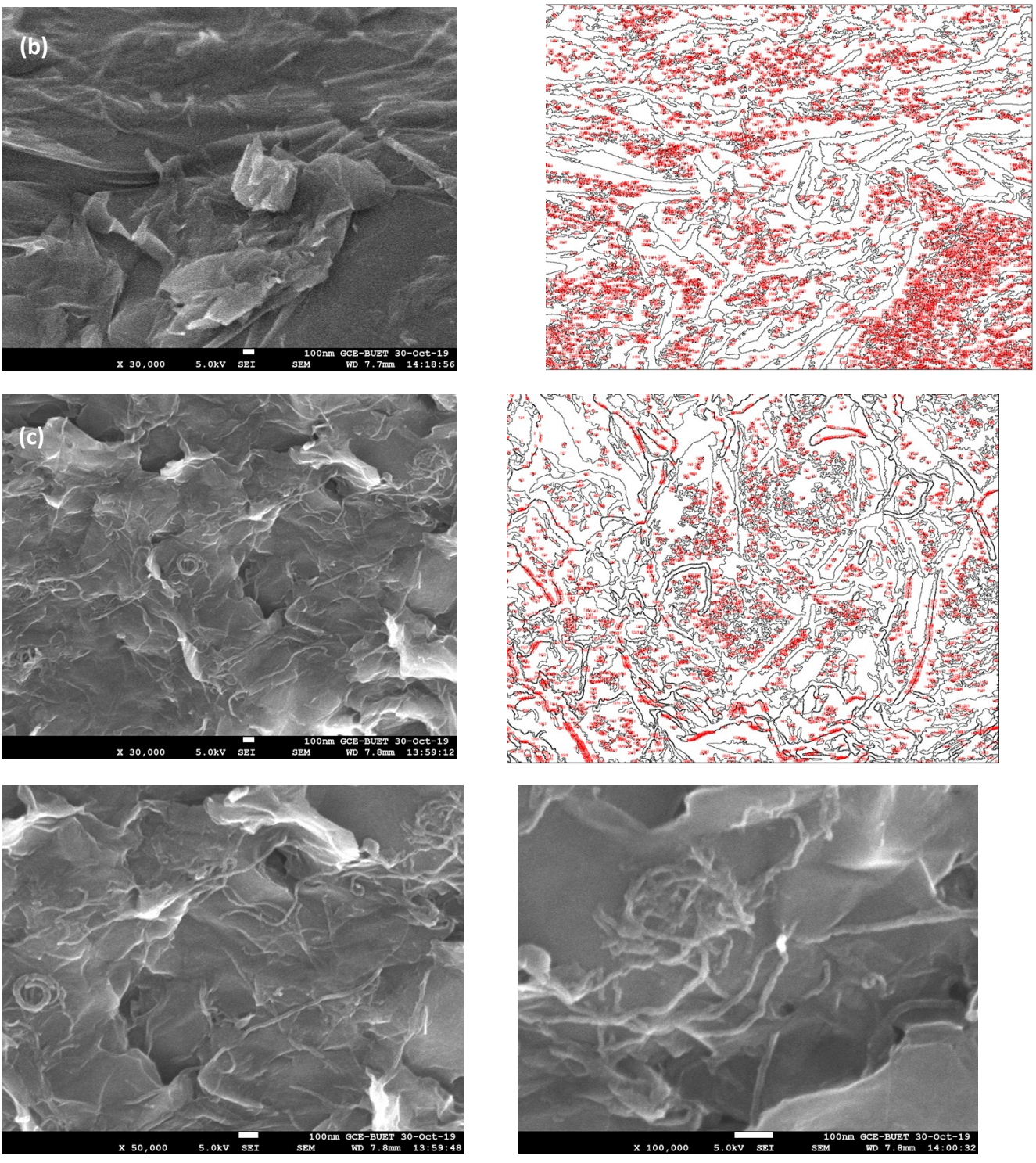

Fig. SI3: Experimental FESEM image of **(a)** GMCNT-15, **(b)** GMCNT-30. Right side images are the corresponding mapped images.

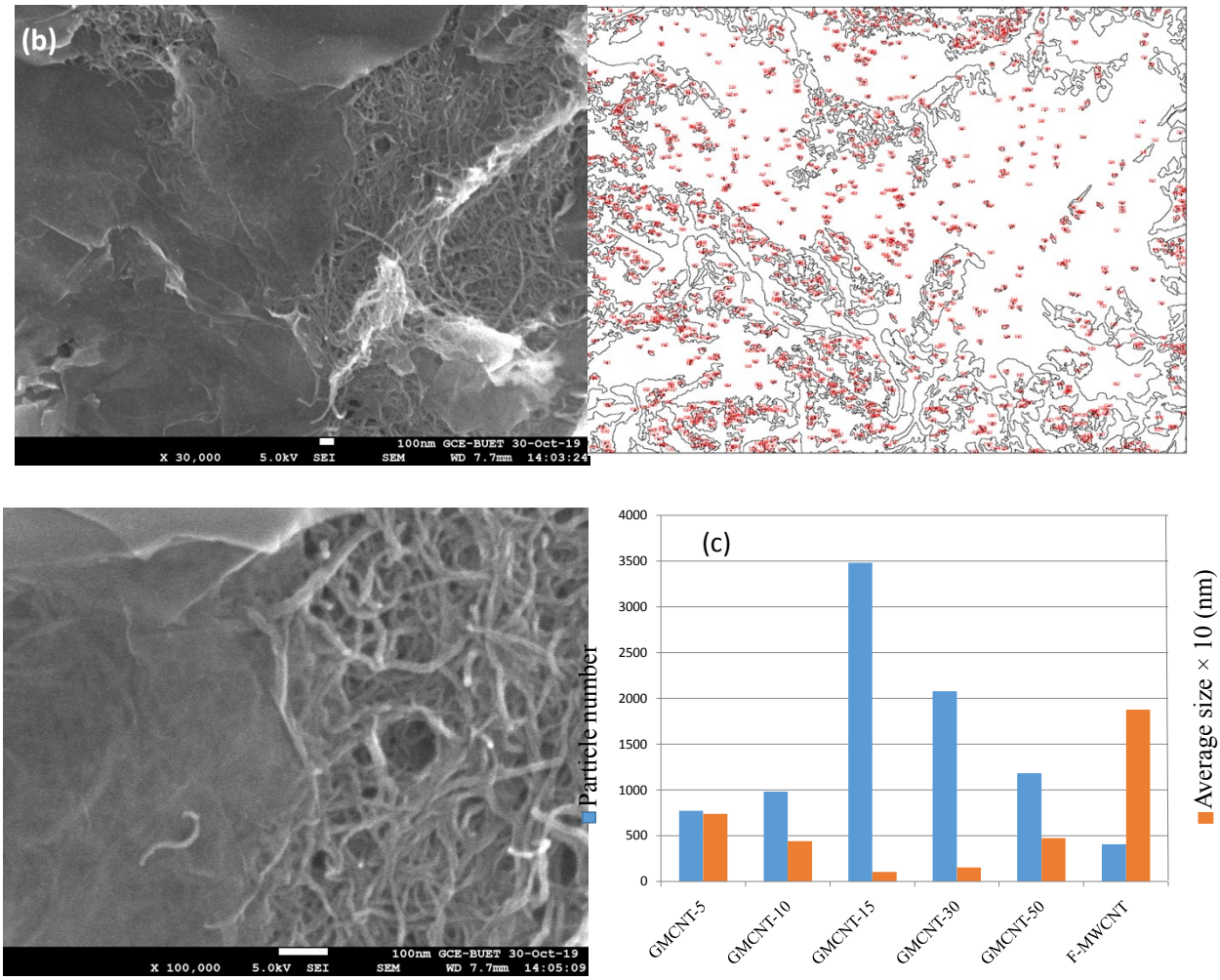

Fig. SI4: Experimental FESEM image of **(a)** GMCNT-50 and **(b)** high magnification image of aggregated MWCNT in GOM. **(c)** Summary of particle count and particle size of composites.

5. X-ray powder diffraction (XRD) study

XRD patterns of all powder samples were recorded with a Philips PW-1830 X-ray generator operating at 40 kV, 40 mA and XDC-700 Guinier Hägg focusing camera using Cu $K\alpha_1$ radiation (λ = 1.540598 Å). X-ray was exposed for 15 min on an image plate for each sample. Image pate is a laser activated sheet which was scanned using HD-CD 35 NDT/CR 35 NDT scanner to get intensity versus line position (mm) pattern. The XRD pattern of intensity versus 2ϑ was found after conversion of line position from millimeter to 2ϑ from the geometry of camera and Bragg equation. The crystallite size (D) of the composites was calculated using Scherrer's equation (SI-6) as summarized in Table ST-1:

$$D = \frac{0.9\,\lambda}{\beta \cos\theta} \qquad \text{(SI-6)}$$

where, β is full width at half maximum (FWHM in radian) of a peak, ϑ is the angle in radian and λ is the wavelength (1.540598 Å) of incident X-rays.[S6] In eq. SI-6, the Scherrer constant (*K*) was chosen as 0.9. Langford and Wilson have reported that breadth of diffractogram that has been defined in several ways, e.g., FWHM, depend on the shape, size and crystal planes.[S7] A distribution of crystallite sizes affect the various measures of breadth in different ways, and thus alter the various Scherrer constants.[S7] If the crystallites are more or less uniform in shape, they may not be uniform in size and the different Scherrer constants result in different size of crystallite. For determining an 'true crystallite size' the actual value of *K* of the crystal system should be chosen. However, for simplicity of our study, the same value of *K* was chosen to determine the size of crystallites of the compounds studied.

Table ST-1: Crystallinity and crystallite size of various components of the composites.

Composites	% Crystalinity	Crystallite size of MWCNT (nm)	Crystallite size of MnO_2 (nm)
GMCNT-5	90	13.5	7.33
GMCNT-10	27	0.35	1.73
GMCNT-15	18	0.22	1.33
GMCNT-30	30	0.27	1.07
GMCNT-50	48	4.42	0.93

6. Determination of crystal structure of GMCNT-5 composite

By using Match 3! (2003-2018 CRYSTAL IMPACT, Bonn, Germany), Endeavour, Diamond 4 software, the crystal structure of GMCNT-5 was typically calculated. The theoretical XRD patterns for calculated structure were determined by Endeavour software (version: 3.6.2.121, 2003-2018 CRYSTAL IMPACT, Bonn, Germany) which are shown in Fig. SI5. The XRD patterns of experimental and theoretical GMCNT-5 are quite similar. The structure obtained from Endeavour software is shown in Fig. SI6 and has triclinic crystal structure with same parameters. The data extracted for the refined crystal structure of GMCNT-5 are shown as follows:

Formula sum	C24 O84 Mn84
Formula weight	6246.797
Crystal system	Triclinic (anorthic)
Space group	P 1
a (Å)	10.296
b (Å)	10.296

c (Å)	3.5186
Density (g/cm^3)	Cal. 27.807

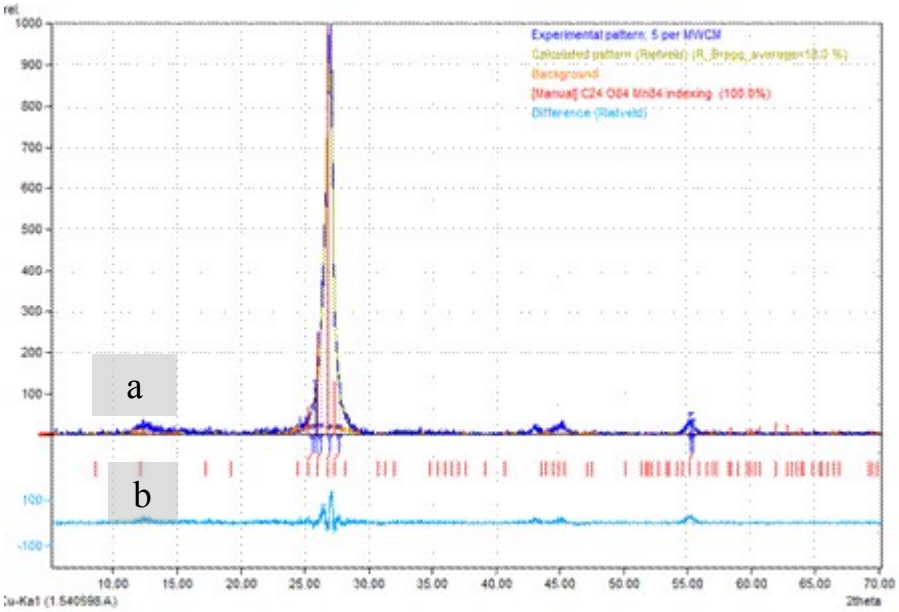

Fig. SI5: XRD patterns of GMCNT composite: **(a)** Experimental and **(b)** Calculated.

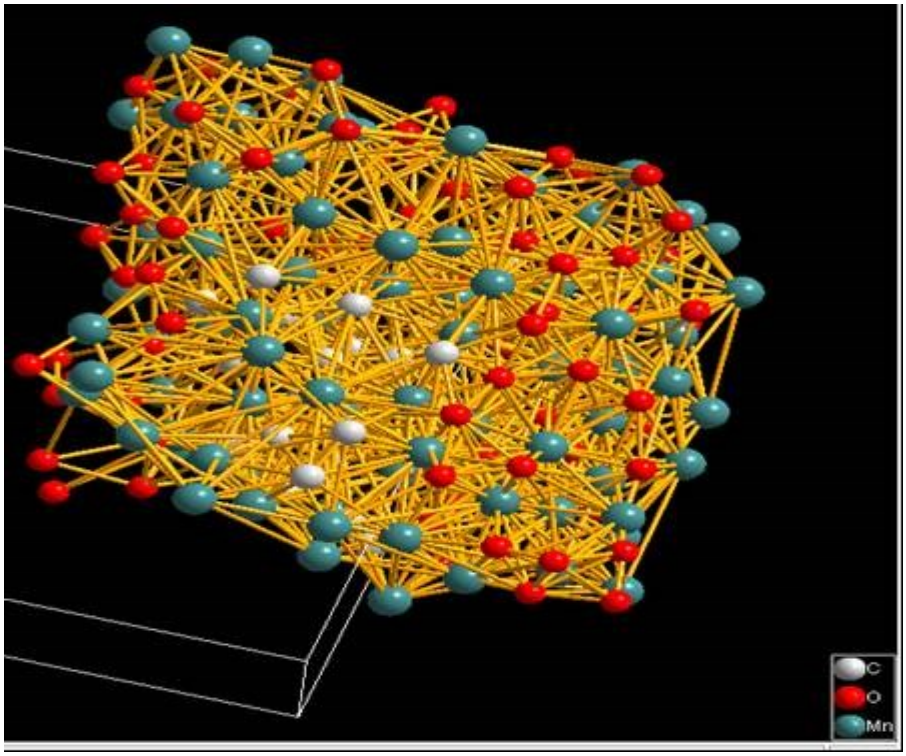

Fig. SI6: Optimised crystal structure of GMCNT composite.

7. Effect of amount of composites loading on specific capacitance (C_{sp})

The amount of active material loaded on the current collector is very important for the practical application like battery or supercapacitor system. The GCD responses and the relationship between the C_{sp} value and the amount of active material deposited on the electrode surface are shown in Fig. SI7. As the amount of loaded material increases, the coating thicknesses per substrate area increased accordingly. However, with increasing the thickness the C_{sp} decreased nonlinearly. This decrease in the C_{sp} is owing to the increasing thickness and hence decreasing effective contact between the reactive surface of the electrode and electrolyte ion.[S8]

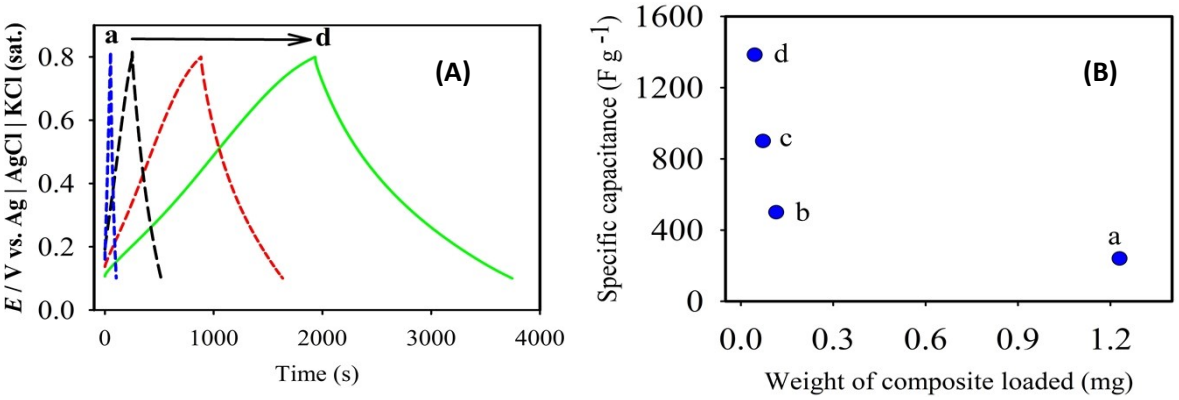

Fig. SI-7: Effect of loading amount of GMCNT-15 composites. **(A)** GCD responses measured by applying a constant current density of 0.5 A g^{-1} and **(B)** Variation of C_{sp} against the amount of composite loaded.

References

S1 Q. Cheng, J. Tang, J. Ma, H. Zhang, N. Shinya and L. C. Qin, *Carbon Y.*, 2011, **49**, 2917–2925.

S2 D. P. Dubal, D. S. Dhawale, R. R. Salunkhe and C. D. Lokhande, *J. Electrochem. Soc.*, 2010, **157**, A812.

S3 S. Sadhukhan, T. K. Ghosh, D. Rana, I. Roy, A. Bhattacharyya, G. Sarkar, M. Chakraborty and D. Chattopadhyay, *Mater. Res. Bull.*, 2016, **79**, 41–51.

S4 D. C. Marcano, D. V. Kosynkin, J. M. Berlin, A. Sinitskii, Z. Sun, A. Slesarev, L. B. Alemany, W. Lu and J. M. Tour, *ACS Nano*, 2010, **4**, 4806–4814.

S5 J. D. Núñez, A. M. Benito, S. Rouzière, P. Launois, R. Arenal, P. M. Ajayan and W. K. Maser, *Chem. Sci.*, 2017, **8**, 4987–4995.

S6 D. M. Smilgies, *J. Appl. Crystallogr.*, 2009, **42**, 1030–1034.

S7 J. I. Langford and A.J.C Wilson, *J. Appl. Cryst.*, 1978, **11**, 102–113.

S8 C. J. Hung, P. Lin and T. Y. Tseng, *J. Power Sources*, 2013, **243**, 594–602.